engineering proceedings

MDPI

Proceeding Paper

Auto-Tuning Sync in the Acoustic Emission Mapping for CFRP Milling †

Paulo Vitor Pereira de Oliveira [1,*], Lucas Zanasi Matheus [1], Fabio Romano Lofrano Dotto [1], Pedro de Oliveira Conceição Junior [1], Alessandro Roger Rodrigues [2] and Dennis Brandao [3]

[1] Departament of Eletrical and Computer Engineering, São Carlos School of Engineering (EESC), University of São Paulo (USP); São Carlos, São Paulo 13566-590, Brazil; lucaszanasi@usp.br (L.Z.M.); fabio.dotto@usp.br (F.R.L.D.); pedro.oliveiracjr@usp.br (P.d.O.C.J.)

[2] Department of Mechanical Engineering, São Carlos School of Engineering (EESC), University of São Paulo (USP); São Carlos, São Paulo 13566-590, Brazil; roger@sc.usp.br

[3] Department of Information Engineering, University of Brescia—UNIBS, 25121 Brescia, Italy; brandao@unibs.it

* Correspondence: paulo_vitor@usp.br

† Presented at The 11th International Electronic Conference on Sensors and Applications (ECSA-11), 26–28 November 2024; Available online: https://sciforum.net/event/ecsa-11.

Abstract: In milling applications of CFRP (Carbon Fiber Reinforced Polymer) composites, acoustic emission sensors employing piezoelectric transducers have been used to generate acoustic maps. These maps are crucial for monitoring the condition of both the tool and the workpiece, providing a visual analysis of the tool-workpiece interaction that facilitates decision-making by the operator in case of failures. This study introduces a technique, implemented in the Matlab software, that uses the image generated by the acoustic map to perform automatic alignment during the map's production, eliminating the need for an external synchronization signal.

Keywords: milling; acoustic map; piezoelectric transducer; IoT sensor

Citation: de Oliveira, P.V.P.; Matheus, L.Z.; Dotto, F.R.L.; de Oliveira Conceição Junior, P.; Rodrigues, A.R.; Brandao, D. Auto-Tuning Sync in the Acoustic Emission Mapping for CFRP Milling. *Eng. Proc.* **2024**, *6*, x. https://doi.org/10.3390/xxxxx

Academic Editor(s):

Published: 26 November 2024

1. Introduction

Driven by the growth of Industry 4.0, the advancement of machine integration and manufacturing automation through IoT systems are progressing rapidly, as the new factories' layout tendency is aimed to remote centralized control of the machinery [1,2]. In this context, the scaling complexity of the production process grows the necessity for systems with higher self-management, which requires larger and more accurate amounts of data.

The expansion of milling operations in new industries also shares these prerequisites; consequently, more studies regarding Tool Condition Monitoring, feature extraction, and failure diagnosis (commonly relying on artificial intelligence, deep learning, and acoustic emissions) are being developed in this area. In this subject, there are studies like [3] that explore the creation of acoustic maps using a low-cost piezoelectric diaphragm sensor, identifying specific frequency bands for filtering acoustic emission (AE) signals, resulting in significant improvements in image quality and clarity. Moreover, the approach in [4] develops a wear monitoring method for CNC machine tools using the 2σ-RMS method and Densenet, while [5] proposes a wear monitoring strategy employing a combination of multilayer perceptron (MLP), radial basis function neural network (RBFNN), wavelet neural network (WNN), and response surface methodology (RSM), and also [6] proposes an online monitoring method for tool wear based on Gated Recurrent Unit Convolutional Neural Network (GRU-CNN). In this paper, it is proposed an Auto-Tuning Sync in the Acoustic Emission Mapping algorithm, implemented in the Matlab software. This method utilizes RMS calculus to determine the concentration of energy in each map section and then uses standard deviation to evaluate the alignment of acoustic energy peaks in said

map with the physical phenomenon, followed by comparing the resulting parameters of each syncing frequency and automatically selecting the optimal spindle frequency.

2. Methodology

2.1. Data Acquisition System

In this study, a ROMI Discovery 400 CNC milling machine was employed, equipped with a 4-edge cutting end mill, specifically the model 50° d10*D10*100L 4F, designed for machining a CFRP plate. To gather data, a data acquisition system was utilized, comprising an acoustic emission sensor coupled with an oscilloscope capable of capturing data at a rate of 1 MS/s. The sensor was installed on the bracket where the CFRP plate was mounted during the milling process. Data gathering was initiated by a trigger signal, activated at the moment the tool made contact with the workpiece, and the data were collected and stored for 3.5 s for subsequent processing. The milling procedure was set up for a downward helical movement with a 'h' pitch and 'R' radius, resulting in the creation of a hole in the CFRP plate, with the tool's spindle speed set at 7000 rpm. In the development of the acoustic map, each row was designed to represent three complete revolutions of the tool around its axis, while the columns indicated the total duration of the milling tests on the material, thereby composing a two-dimensional image. The pixels of this image were generated using RMS statistics; specifically, for each RMS point, 27 samples of pure acoustic emission (AE) signal were processed, achieving a resolution of 0.1 mm on the map. Figure 1 shows the appearance of the used milling cutter (a), the arrangement of the cutting edges (b), and the helical movement of the milling cutter during the machining process of the CFRP plate.

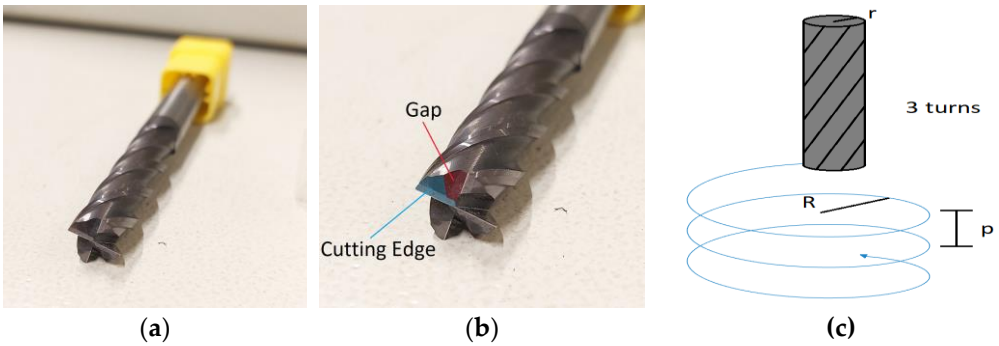

Figure 1. 4 edges 50° d10*D10*100L 4F End Mil milling cutter: (**a**) Inside the packaging; (**b**) Cutting edges; (**c**) helical movement of the milling cutter.

The parameters for the milling process were carefully set to allow for clear visualization of the tool's cutting edges on the acoustic map. The cutting speed and feed per edge were adjusted so that the distribution of forces generated would result in an appropriate acoustic response, facilitating visual separation of the edges on the map. Additionally, the depth of cut, width of cut, and feed rate of the tool were optimized to ensure that the duration of the tests did not exceed the stipulated time of 3.5 s.

2.2. Synchronization Method

For acoustic mapping, the use of an external synchronization signal is common [3]; however, this method requires an additional channel for acquiring the signal, leading to a more complex and expensive data acquisition system. To avoid the need for an external synchronization signal, it was observed that based on the conditions established in Section 2.1, a correction index can be derived from the misalignment of cutting edges seen in the acoustic map. This index can estimate the spindle rotation without relying on an external synchronization signal.

Due to the geometry and translational movement of the cutting tool, the pressure exerted by the cutting edge on the CFRP with each tool revolution results in an alternance of peaks in the acoustic emission signal. These variations appear as cyclical vertical bands on the acoustic map, which show an inclination due to a lack of synchronization between the programmed spindle rotation speed and the actual speed. From this misalignment, a correction index can be obtained that enables the accurate estimation of the actual spindle rotation speed, thereby eliminating the need for an additional external synchronization signal.

The algorithm proposed in this work is detailed in the flowchart presented in Figure 2. This flowchart shows that, starting from an acoustic emission signal captured during the process, a fifth-order Butterworth band-pass filter is applied, adjusted to the frequency range of 10 kHz to 180 kHz. Subsequently, an acoustic map is generated based on a spindle speed programmed into the CNC machine during milling. Although the machine allows for the configuration of this parameter, there is a noticeable discrepancy between the programmed value and the actual parameters due to errors introduced by the frequency inverter and the mechanical characteristics of the process. As a result, a misaligned acoustic map is produced.

From this misaligned map, the detection of energy peak strips is calculated using root mean square (RMS) statistics, standard deviation, and error estimation. Based on this error, a new actual spindle speed is calculated, which can be used to correct and align the acoustic map, eliminating the need for an external synchronization signal.

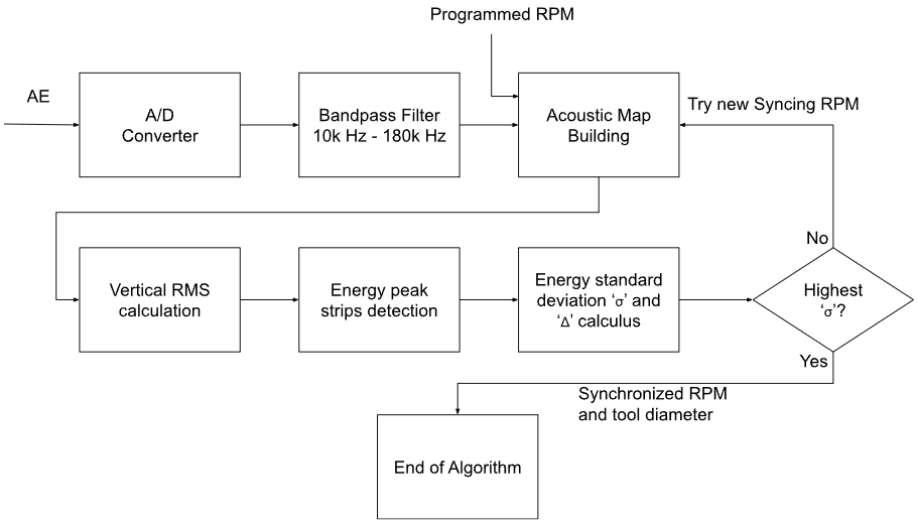

Figure 2. Algorithm flowchart.

The algorithm developed in Matlab operates in four main steps: calculating the RMS for each column of the map, identifying energy peaks using an envelope function to locate peaks and valleys, calculating the standard deviation of the mean energy to measure the energy dispersion across the samples, and calculating the mean separation between peaks, which corresponds to the number of samples between the cutting-edge activities, later converted to millimeters. The mean peak separation ($\bar{\Delta}$) is calculated by the following equation:

$$\overline{\Delta} = \frac{m_r}{N} \sum_{n=1}^{N-1} |(xpeak_n - xpeak_{n+1})| \quad (1)$$

where $xpeak_n$ is the x coordinate of the n^{th} peak; N is the total number of peaks and $m_r = 0.1$ mm/sample is the map resolution.

Figure 3 illustrates the distance between the cutting edges of the tool and the vertical bands in the synchronized acoustic map, which are equidistantly spaced using the $\bar{\Delta}$ coefficient.

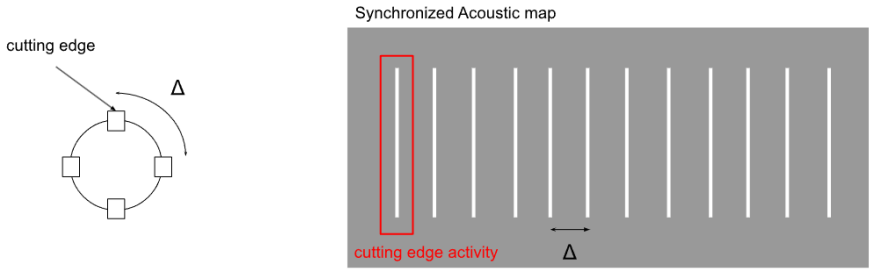

Figure 3. Cutting edges of the tool (**a**) and synchronized acoustic map (**b**).

3. Results and Discussion

For the experimental tests, helical hole milling was performed on CFRP plates, with the tool rotation speed set to 7000 rpm on the CNC machine. Several acoustic maps were generated using the technique developed by [3]. Based on this programmed rotation speed, the previously described method was applied (Figure 2). Figure 4 shows the conditions of the acoustic map obtained both with and without the alignment of the synchronization signal. Despite the speed configured on the machine, the technique allowed for the determination of the actual spindle speed, which was 6993 rpm. Additionally, the vertical bands on the map, corresponding to the tool's cutting edges, were clearly visible that is, 3 revolutions of the tool with 4 cutting edges each, totaling 12 vertical bands. Three revolutions per line were considered in the map to ensure better point distribution and clearer visualization of the acoustic map. The vertical axis of the acoustic map represents the milling time during the perforation of the CFRP plate.

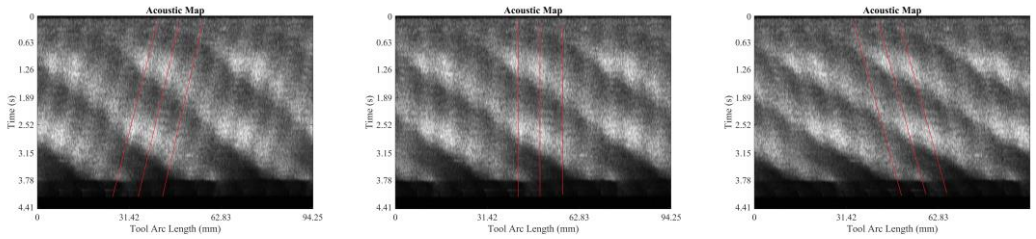

Figure 4. Generated acoustic maps for 6988 RPM, 6993 RPM, and 7000 RPM.

The signals resulting from the steps to obtain the RMS values from the acoustic map rows and the detection algorithm are shown in Figure 5. In this figure, the unsynchronized map, with a rotation speed of 6988 RPM, is compared to the synchronized map, which was realigned by the implemented algorithm to achieve 6993 RPM. Additionally, Figure 5 highlights the spacing between peaks, corresponding to the tool's cutting edges, as well as the increase in mean energy standard deviation, indicating precise synchronization. This adjustment allows for the generation of a synchronized map without the need for external synchronization signals.

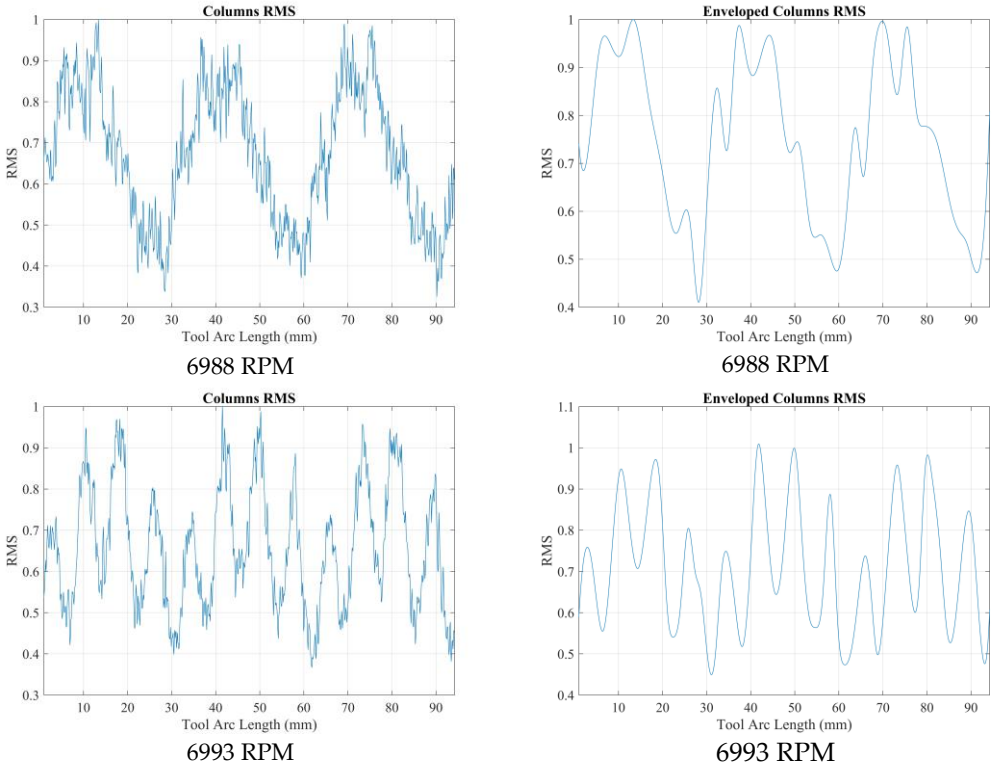

Figure 5. RMS statistics applied to the acoustic map rows and peak detection for synchronizing the tool's cutting edges: 6988 RPM (unsynchronized) and 6993 RPM (synchronized).

Table 1 presents a summary of the parameters obtained through the implemented technique, demonstrating the increase in the mean energy standard deviation (σ) when acoustic map synchronization is achieved. It also shows the average peak separation (Δ'), which reflects the physical spacing between the cutting edges of the milling tool. Ideally, this value should be close to 80 points, corresponding to an arc length between edges of approximately 7.85 mm.

Table 1. Operation parameters.

Syncing Frequency	Mean Energy Standard Deviation 'σ'	Mean Peaks Separation 'Δ'
6988 RPM	1.782787	85.200000
6993 RPM	7.020648	79.818182
7000 RPM	1.218722	73.333333

Another point to consider is that the higher the mean standard deviation of the RMS spectrum, the more concentrated the energy becomes in a narrower band, unlike the tested synchronization frequencies of 6988 RPM and 7000 RPM, where the energy is dispersed across a wider bandwidth.

Additionally, the 'σ' ratio was nearly four times higher (highlighting its discrepancy compared to the deviation of nearby synchronization frequencies), and the relative error between the calculated 'Δ' and the theoretical 'Δ' was 1.63%.

4. Conclusions

In this study, an automatic synchronization algorithm for acoustic maps obtained from acoustic emission signals was proposed and implemented in Matlab. Experiments conducted on a CNC machine generated acoustic maps that described the milling process of CFRP plates, revealing that the actual tool rotation speed diverged from the

programmed speed, leading to desynchronization. The results demonstrated that the algorithm was effective in distinguishing the synchronized map from the unsynchronized ones and in estimating the distance between the tool's cutting edges.

These findings suggest that, under specific machining conditions, the use of an external synchronization signal for constructing the acoustic map is unnecessary, thereby simplifying the data acquisition system, making it more economical, and computationally less complex. This advancement represents a significant contribution to the development of embedded IoT sensor solutions aimed at Industry 4.0.

For future research, it is recommended to analyze acoustic maps generated under broader conditions, such as the use of different milling cutters, other machining conditions, tests with lubricating fluids, and various material types, as well as applying the algorithm to other machines and similar processes, such as grinding and drilling.

Author Contributions: Conceptualization, F.R.L.D. and P.V.P.d.O.; methodology, P.V.P.d.O.; software, P.V.P.d.O. and F.R.L.D.; validation, P.d.O.C.J. and A.R.R.; formal analysis, F.R.L.D. and P.V.P.d.O.; investigation, D.B. and L.Z.M.; resources, D.B., A.R.R. and L.Z.M.; data curation, F.R.L.D.; writing—original draft preparation, P.V.P.d.O.; writing—review and editing, P.V.P.d.O. and F.R.L.D.; visualization, D.B., P.d.O.C.J. and A.R.R.; supervision, F.R.L.D.; project administration, F.R.L.D.; funding acquisition, F.R.L.D. All authors have read and agreed to the published version of the manuscript.

Funding: This research was funded by Pro-Rectory of Research and Innovation of the University of São Paulo under grant: #22.1.09345.01.2, and the São Paulo Research Foundation, under grant #2024/01374-6.

Institutional Review Board Statement: Not Applicable.

Informed Consent Statement: Not Applicable.

Data Availability Statement: Dataset available on request from the authors.

Acknowledgments: The authors would like the University of São Paulo (USP) and the University of Brescia (UNIBS) for the opportunity to carry out and publish the research.

Conflicts of Interest: The authors declare no conflicts of interest.

References

1. Chen, J.; Zhang, F.; Li, Y. Sound-Based Real-Time Scrap Falling State Monitoring in the Shearing Process of Wide Heavy Plate Mill. *IEEE Sens. J.* **2023**, *23*, 17092–17102. https://doi.org/10.1109/JSEN.2023.3284517.
2. Duo, J.-B. A new model for intelligent steel mill central control and management. *Sci. Technol. Inf.* **2021**, *1*, 1–3.
3. Dotto, F.R.L.; Aguiar, P.R.; Alexandre, F.A.; Lopes, W.N.; Bianchi, E.C. In-Dressing Acoustic Map by Low-Cost Piezoelectric Transducer. *IEEE Trans. Ind. Electron.* **2020**, *67*, 6927–6936. https://doi.org/10.1109/TIE.2019.2939958.
4. Song, H.; Gao, H.; Guo, L.; Li, Y.; Dong, X. CNC Machine Tool Wear Monitoring Based on Densely Connected Convolutional Networks. In Proceedings of the 2020 Prognostics and Health Management Conference (PHM-Besançon), Besancon, France, 4–7 May 2020; pp. 36–41. https://doi.org/10.1109/PHM-Besancon49106.2020.00013.
5. Ong, P.; Lee, W.K.; Lau, R.J.H. Tool condition monitoring in CNC end milling using wavelet neural network based on machine vision. *Int. J. Adv. Manuf. Technol.* **2019**, *104*, 1369–1379. https://doi.org/10.1007/s00170-019-04020-6.
6. Chaowen, Z.; Jing, J.; Chi, C. Research On Tool Wear Monitoring Based On GRU-CNN. In Proceedings of the 2021 6th International Conference on Intelligent Computing and Signal Processing (ICSP), Xi'an, China, 9–11 April 2021; pp. 729–733. https://doi.org/10.1109/ICSP51882.2021.9408717.